Appendix A - Detailed methods

2.3. Small- and wide- angle X-ray scattering

2.3.1. Experimental set up

Small- and wide- angle X-ray scattering (SAXS/WAXS) experiments were performed at the mySpot beamline at the BESSY II synchrotron radiation facility (HZB, Helmholtz-Zentrum Berlin für Materialien und Energie, Berlin, Germany). The wavelength was 0.826 Å (energy of 15 kev), the beam was 30 µm large and the scattering patterns were collected on a 2D detector (MARCCD 225, marusa, Evanston) with 73.242 x 73.242 μm^2 pixel size and 3072 x 3072 pixels. The sample-detector distance was 0.310 m. The exposure time was 10 s per scan point. The scan step was 100 µm. Measurements were calibrated using crystalline silver behenate powder.

2.3.2. Data analysis

The SAXS signal arises from electron density differences between the HAP nano platelets and the organic collagen matrix. The shape of the two dimensional (2D) SAXS signal provides information on the average degree of alignment of the mineral platelets within the irradiated sample volume. Thus, an anisotropic 2D SAXS signal indicates a high organization of the mineral platelets in one specific orientation (Figure 1 A), whereas an isotropic 2D SAXS signal is due to randomly oriented HAP particles (Figure 1 B). However, if the mineral particles (with their long dimension) are not parallel to the beam, an isotropic SAXS signal can also result from out-of plane particle orientation [1, 2].

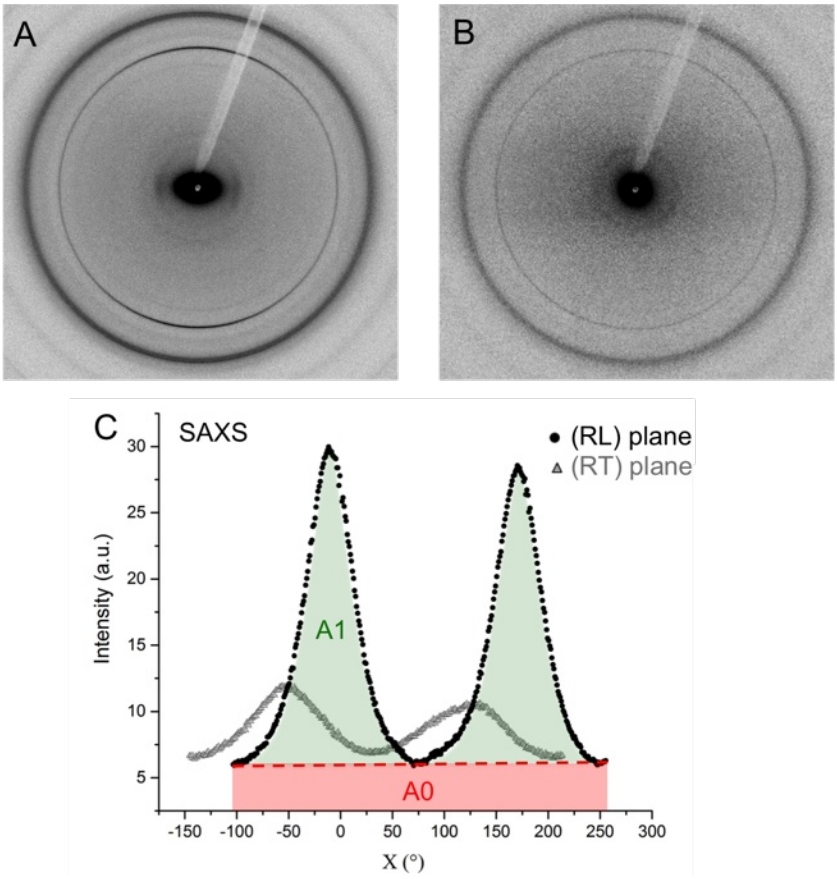

Figure 1. A) Averaged SAXS/WAXS 2D pattern of the (RL) plane profile from R=5 to 20 mm, B) averaged SAXS/WAXS 2D pattern of the (RT) plane from R=0 to 3 mm and C) radial integration of the SAXS signals of the (RL) and (RT) sections showing the area A1 and A0 for the calculation of the ρ-parameter for the (RL) plane.

A more quantitative analysis can be done by calculating the ρ-parameter [3, 4]. The ρ-parameter describes the degree of alignment of the mineral particles i.e. the percentage of HAP crystals presenting the same orientation in the analyzed volume. It is calculated from the radial integration of the SAXS signals (Fig. 1C) by $\rho = A1/(A1+A0)$ where A1 represents the percentage of organized HAP particles having a preferred orientation and A0 the percentage of randomly oriented HAP particles.

The ρ-parameter does not, however, provide any information concerning out of plane orientations. Therefore, a ρ-parameter of 0 means that HAP minerals are randomly

oriented or that they are oriented but with their axis along the long dimension perpendicular to the beam. A ρ-parameter equal to 100% means that HAP particles present a preferred orientation.

Finally, where the mineral particles are sufficiently organized (ρ≥ 40%), it is possible to assess the preferred orientation of their c-axis by the previous radial integration of the SAXS signal (Figure 1 C) or of the (002) reflection of the HAP crystals seen in the 2D WAXS pattern. The intensity distribution of this reflection shows the probability of HAP c-axes to be oriented in a given direction χ_{max} (maximum of the intensity of the χ-distribution), which is the c-axes projection in the sample plane with respect to the vertical of the samples. In the case of the (RL) section, the sample was aligned with the (L) axis perpendicular to the beam and in the case of the (RT) section, the sample was aligned with the (T) axis perpendicular to the beam. Therefore, $\chi_{max(RL)}$ is the projected angle between the MCF axis and the tusk axis and $\chi_{max(RT)}$ is the projected angle between the MCF long axis and the (T) axis.

The ρ-parameter and χ_{max}-angle were calculated after having respectively integrated the 2D SAXS and WAXS signals as a function of the azimuthal angle using the software Fit2D (Hammersley et al., 1996) and Autofit, custom-made software (Max Planck Institute of Colloids and Interfaces, Potsdam, Germany).

For the (RT) plane, $\chi_{max(RT)}$ values were extracted from 2.6 to 3 mm from the cement. The reported are reported in the table below. Values from 2.6 to 3 mm are missing because the section broke close to the cement due to low thickness.

Position from cement (R in mm)	ρ-parameter (%)	χmax (RT) (°)
2.6	42	56
2.65	44	53
2.7	46	46
2.75	48	54
2.8	51	46

2.85	51	56
2.9	54	52
2.95	49	44
3	42	40
	Average	50
	SDV	6

2.4. Cross-polarized light and scanning electron microscopy

Samples were observed by cross-polarized light microscopy (CPL, DM RXA2 Leica, Bensheim, Germany, with air objective 2.5x numerical aperture of 0.07) in which the polarizer and analyzer were fixed perpendicularly to each other (cross-polarized light). The microscope's goniometric stage allows rotation of the specimen with respect to the crossed polarizers. The intensity of the transmitted light depends on the collagen content, its degree of alignment, on the mineral fraction and on the orientation of the section. Therefore, we demineralized the sections (see 2.2 for details). As seen by the WAXS pattern of the (RL) sections before and after removal of the mineral part, the demineralization process was successful. The mineralized section shows the typical HAP signals with the (002), (211), (112) and (300) reflections whereas the demineralized section does not show them.

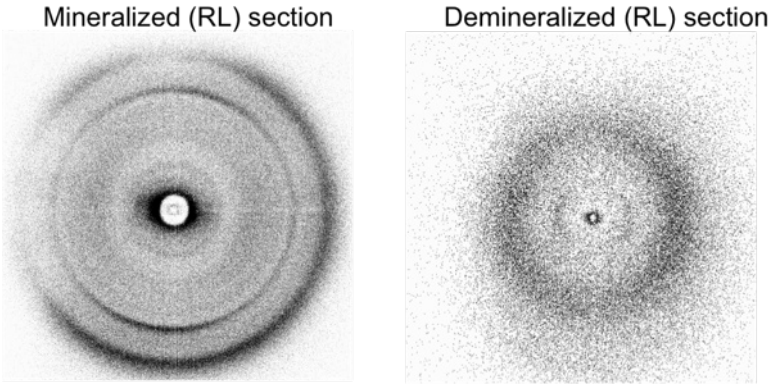

The demineralized sections with controlled thicknesses (~70 μm) were measured at various angles from the crossed polarizers in order to determine the collagen fibers (CF) orientations by distinguishing extinction and illumination positions. Due to the

interaction between light and the tissue, the brightest areas will be observed for CF lying in the observation plane (i.e. normal to the light propagation) and oblique (+ or - 45º) to the analyzer and polarizer, while darker regions will correspond to CF oriented perpendicularly to this direction or within the plane but orientated parallel to the direction of either the analyzer or the polarizer. In order to determine if CF in bright areas are oriented at + or - 45º to the crossed polarizer and analyzer, a quartz first-order retardation λ plate was at 45º between the polarizer and analyzer. Indeed, the λ plate allows evidencing CF oriented parallel to the slow axis of the λ plate (blue domains) and CF perpendicular to it (orange domains).

A digital scanning electron microscope (SEM, DSM 962, Zeiss, Oberkochen, Germany) was used for the observations of fractured sections with the secondary electron mode in order to provide topographic contrast. The SEM was set to an accelerating voltage of 20 keV and a working distance of 10 mm was used.

[1] A. Gourrier, W. Wagermaier, M. Burghammer, D. Lammie, H.S. Gupta, P. Fratzl, C. Riekel, T.J. Wess, O. Paris, Scanning X-ray imaging with small-angle scattering contrast, J. Appl. Crystallogr. 40 (2007) S78-S82.
[2] Y.F. Liu, I. Manjubala, P. Roschger, H. Schell, G.N. Duda, P. Fratzl, Mineral crystal alignment in mineralized fracture callus determined by 3D small-angle X-ray scattering, in: G. Ungar (Ed.), Xiv International Conference on Small-Angle Scattering, Iop Publishing Ltd, Bristol, 2010.
[3] P. Fratzl, N. Fratzlzelman, K. Klaushofer, G. Vogl, K. Koller, Nucleation and growth of mineral crystals in bone studied by small-angle x-ray-scattering, Calcif. Tissue Int. 48(6) (1991) 407-413.
[4] P. Fratzl, M. Groschner, G. Vogl, H. Plenk, J. Eschberger, N. Fratzlzelman, K. Koller, K. Klaushofer, Mineral crystals in calcified tissues - a comparative-study by SAXS, J. Bone Miner. Res. 7(3) (1992) 329-334.

Appendix B – Supplementary figures

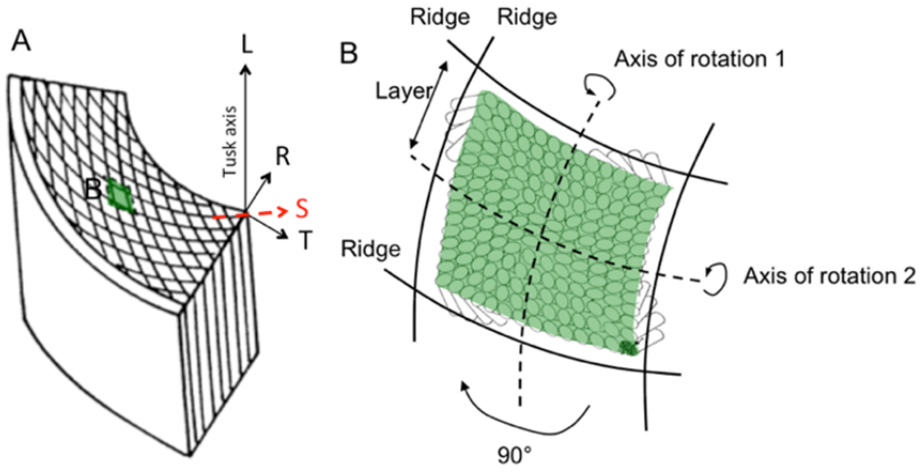

Supplementary Fig. 1. 3D arrangement of the mineralized collagen fibers in elephant ivory proposed by [1]. A) Scheme of a section of ivory with the reference system indicated, the transverse (RT) plane shows the intercrossing ridges of the Schreger pattern and B) rotated plywood like structure showing the two orthogonal axes of rotation following the Schreger lines. Mineralized CF continuously rotate of 90º from one layer to the other and are mainly oblique to the transverse plane apart on top and bottom of the ridges were they are perpendicular to it and therefore aligned to the tusk axis.

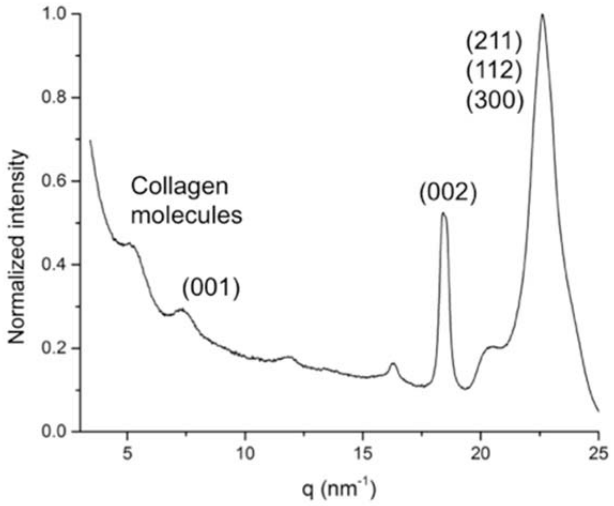

Supplementary Fig. 2. Azimuthal integration of the averaged SAXS/WAXS 2D pattern of the (RL) plane profile from cement to pulp showing the peak corresponding to the spacing between collagen molecules (5.5 nm^{-1}) and the different reflections of the HAP crystals with the characteristic (002) reflection at q = 18.4 nm^{-1}.

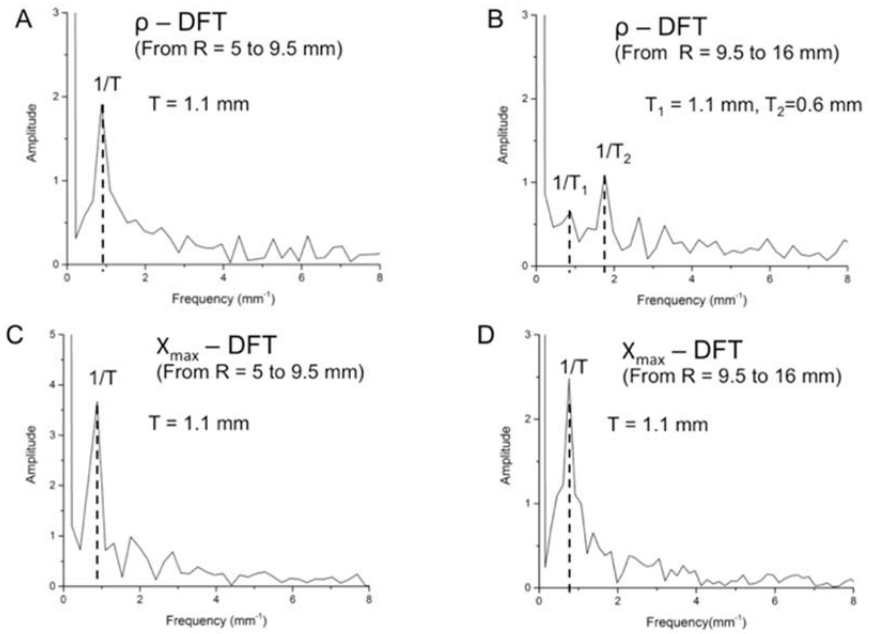

Supplementary Fig. 3. Discrete Fourier Transform (DFT) of the periodic oscillations of the ρ- and χ_{max} profiles in the mid-dentin of the (RL) plane. A) from R=5 to 9.5 mm of the ρ-profile, B) from R=9.5 to 16 mm of the ρ-profile, C) from R=5 to 9.5 mm of the χ_{max}-profile and D) from R=9.5 to 16 mm of the χ_{max}-profile.

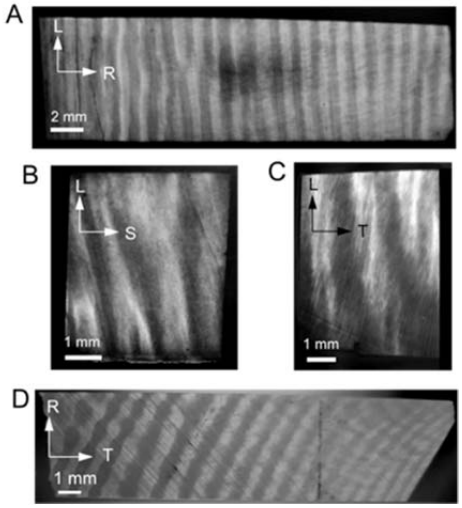

Supplementary Fig. 4. Thin demineralized sections observed under transmitted light and used for cross-polarised microscopy measurements. A) (RL) section cut perpendicular to the rhomboids from cement to pulp, B) (SL) section, C) (TL) section and D) (RT) section.

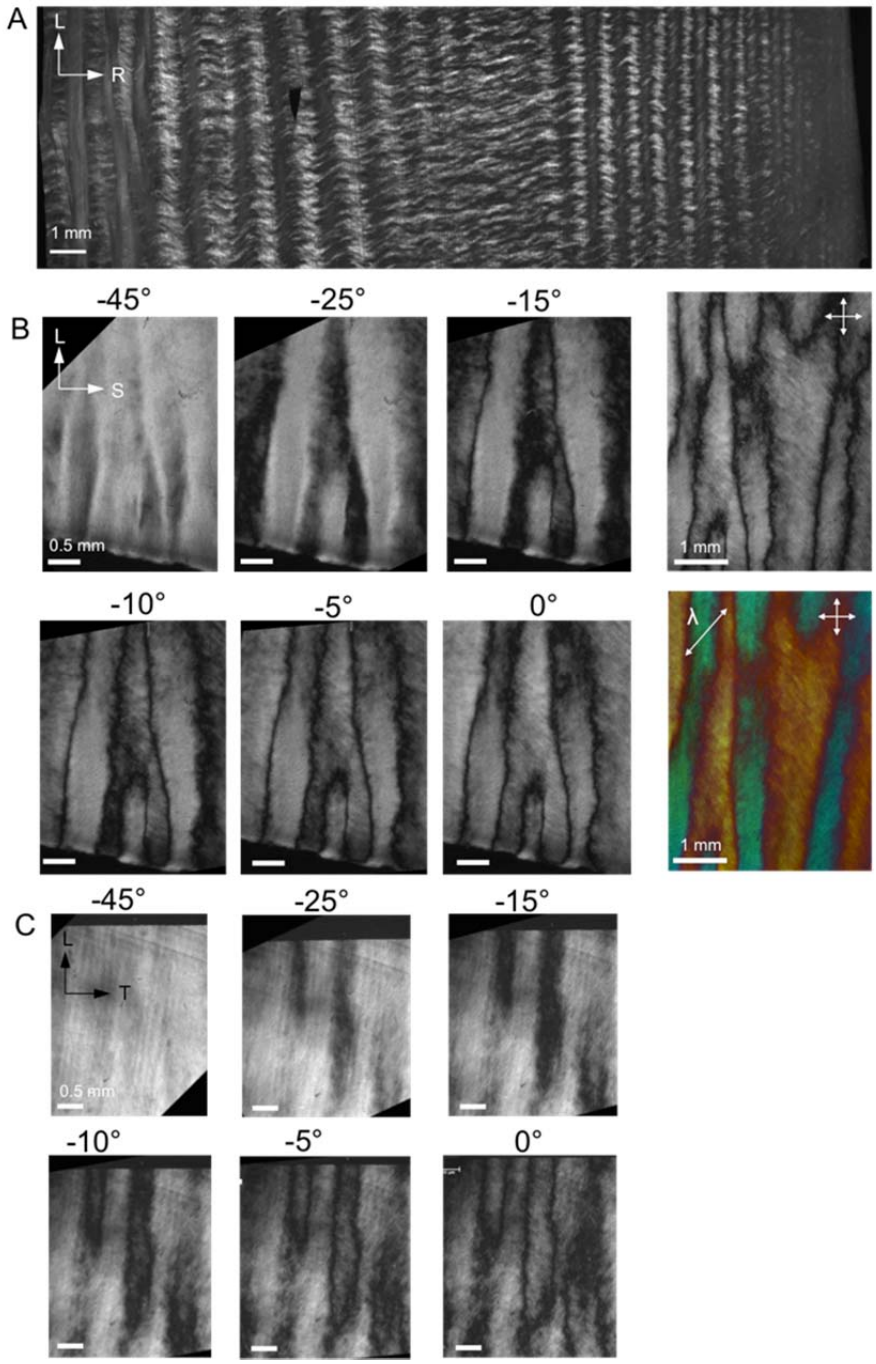

Supplementary Fig. 5. Cross-polarized micrographs of A) the (RL) plane (section used for SAXS/WAXS measurements) from cement to pulp oriented at 5° to the crossed polarizer and analyzer, B) the (SL) section oriented at different orientations and with the additional presence of the λ plate for the orientation at 0° and C) the (TL) plane at different orientations.

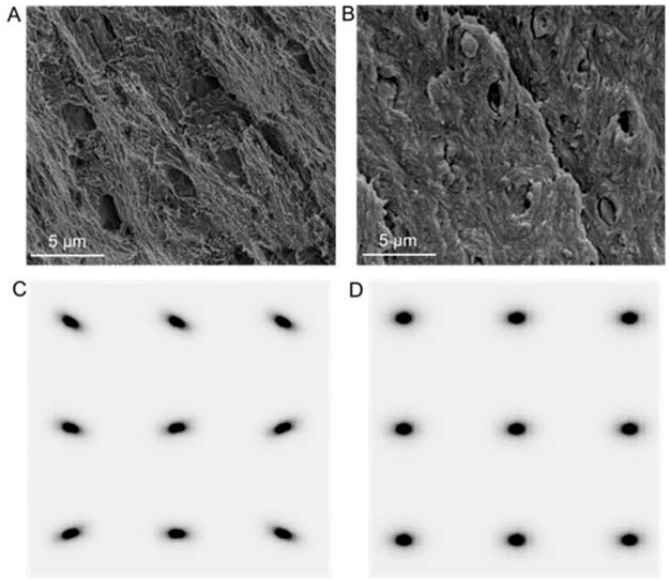

Supplementary Fig. 6. Variation of the MCF orientation in the (TL) plane from cement to pulp. A) SEM image of a fractured section in the mid-dentin which shows MCF aligned in the plane and B) SEM image of a fracture section close to the pulp with MCF distributed around the tubules and having different orientations. C) Anisotropic SAXS signals of a (TL) section in the mid-dentin indicating preferentially aligned MCF and D) Isotropic SAXS signals of a (TL) section close to the pulp revealing less organized MCF than in the mid-dentin.

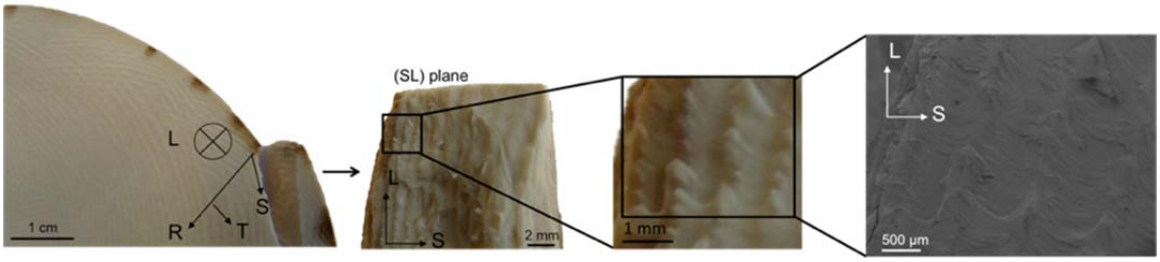

Supplementary Fig. 7. Fractured section along the (SL) plane.

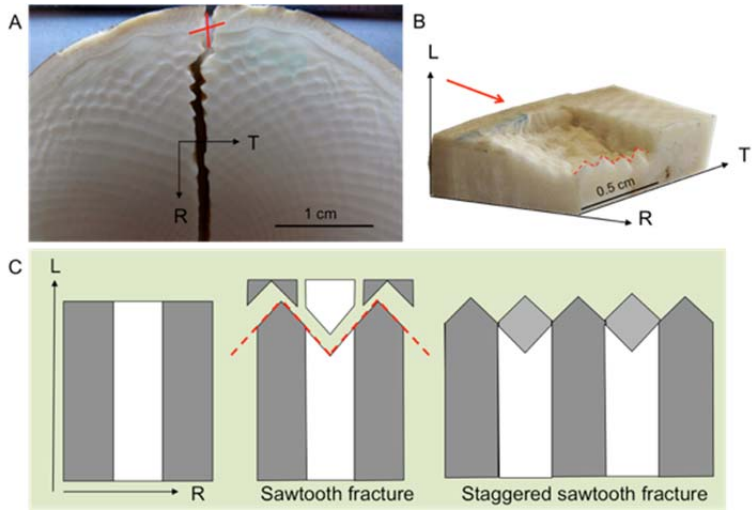

Supplementary Fig. 8. Zizag-like fractures obtained when the percussion was done perpendicular to A) the (RT) plane and B) the (RT) plane. C) Scheme of the possible crack propagation when the percussion is done perpendicular to the tusk axis leading to the sawtooth fracture described in [2].

[1] X.W. Su, F.Z. Cui, Hierarchical structure of ivory: from nanometer to centimeter, Mater. Sci. Eng. C-Biomimetic Supramol. Syst. 7(1) (1999) 19-29.
[2] C.E. Heckel, S. Wolf, Ivory debitage by fracture in the Aurignacian: experimental and archaeological examples, Journal of Archaeological Science 42 (2014) 1-14.